International Journal of Heat and Technology
Vol. 43, No. 5, October, 2025, pp. 1983-1995
Journal homepage: http://iieta.org/journals/ijht

Coupled Model of Economic and Efficiency Performance in Regional Energy Systems Based on Non-Equilibrium Thermodynamics

Lipeng Wang

Shijiazhuang University of Applied Technology, Shijiazhuang 050081, China

Corresponding Author Email: 2003100270@sjzpt.edu.cn

https://doi.org/10.18280/ijht.430538

Received: 28 August 2025
Revised: 18 October 2025
Accepted: 26 October 2025
Available online: 31 October 2025

Keywords:
non-equilibrium thermodynamics, regional energy systems, entropy production rate, economic-efficiency coupling model, LCC, non-equilibrium efficiency, multi-objective optimization

ABSTRACT

In the global energy transition, regional energy systems have become key platforms for achieving carbon reduction targets. The multi-physics coupling characteristics in the energy conversion, transmission, and consumption stages of the system determine its inherent non-equilibrium nature. Traditional studies often analyze system efficiency based on equilibrium thermodynamic assumptions, separating economic evaluation from thermodynamic efficiency analysis, which makes it difficult to precisely quantify the impact of irreversible losses on system performance. Existing research faces two major bottlenecks: The inherent contradiction between equilibrium assumptions and irreversible losses such as entropy production that are common in real systems, and the lack of a quantitative coupling mechanism between economic indicators and non-equilibrium thermodynamic efficiency. To address these issues, this paper integrates core non-equilibrium thermodynamic theories, such as local equilibrium assumptions, entropy production rates, and linear irreversible thermodynamics, with full-life-cycle economic analysis to develop a dynamic coupled model of economic and efficiency performance in regional energy systems. The paper introduces the Non-Dominated Sorting Genetic Algorithm II (IINSGA-II) for multi-objective optimization and combines it with Model Predictive Control (MPC) to enhance the model's adaptability to dynamic operating conditions. The core innovations of this research include three aspects: the introduction of a non-equilibrium efficiency correction index to quantify the effect of non-equilibrium states on traditional efficiency; the establishment of a direct correlation equation between entropy production and full-life-cycle costs (LCC) to reveal the economic cost of thermodynamic irreversibility; and the design of a dynamic coupled adjustment mechanism based on MPC to achieve collaborative optimization of efficiency and cost under load fluctuations. Empirical results show that the proposed model reduces the LCC by 8.9% compared to traditional equilibrium-based models. The calculated non-equilibrium efficiency shows an average absolute error of only 1.05%, with a coefficient of determination of 0.94, demonstrating a significantly higher accuracy than traditional models. Additionally, the impact of non-equilibrium conditions on the coupled optimization results has a weight of 28%, confirming its core role in system optimization. Furthermore, the optimization rate of entropy production in the energy conversion stage exceeds 40%, and the dynamic adjustment error under medium-load fluctuation scenarios can be reduced to a low point near -10, further highlighting the synergistic optimization value of non-equilibrium mechanisms and dynamic adjustment. This paper provides a theoretical framework for the collaborative optimization of thermodynamics and economics in regional energy systems. The proposed model can serve as a quantitative tool for engineering design and energy policy formulation.

1. INTRODUCTION

In the global energy transition driven by the “dual carbon” goals, regional energy systems have become the core platform for integrating distributed energy, regional cooling and heating, and energy storage. Their central role in improving energy efficiency and reducing carbon emissions has been widely confirmed [1, 2]. However, such systems involve the entire chain from energy production to transmission and consumption, and there are multi-physics coupling effects in the temperature, flow, and concentration fields at each stage. This inherent characteristic determines that the system is always in a non-equilibrium operating state [3, 4]. Traditional studies often use equilibrium thermodynamics assumptions to analyze system efficiency. While this assumption simplifies the calculation process, it cannot accurately capture irreversible losses, such as network heat loss and equipment operation under variable conditions, which are commonly present in real-world scenarios. As a result, the efficiency evaluation results deviate significantly from the actual

engineering practices [5-7]. From an engineering practice perspective, the design and operation of regional energy systems always face the core contradiction between improving efficiency and controlling costs. For example, investing in high-efficiency equipment can reduce irreversible losses during operation but will significantly increase initial investment costs [8]; while low-cost equipment selection will lead to a sharp increase in entropy production during operation, raising long-term energy consumption costs [9]. Existing economic and efficiency coupling models are mostly based on static equilibrium assumptions, which ignore the dynamic degradation law of system efficiency with changing operating conditions in non-equilibrium states and fail to consider the nonlinear cost changes caused by the accumulation of irreversible losses. This ultimately leads to optimization solutions that are difficult to implement and achieve the expected benefits in practical applications [10].

The limitations of existing research mainly focus on three aspects, forming gaps that urgently need to be filled. First, there are limitations in the application of non-equilibrium thermodynamics. Current studies mostly apply non-equilibrium thermodynamics theory to analyze the entropy production minimization of single devices such as heat exchangers and heat pumps. While this can support the optimization of individual devices, it lacks a method for characterizing non-equilibrium states at the regional system scale and has not established a quantitative correlation between non-equilibrium and system-wide efficiency, making it impossible to achieve accurate thermodynamic performance evaluation at the system level. Second, the coupling mechanism between economic performance and efficiency has inherent flaws. Traditional coupling models generally associate efficiency and cost by adding weighted objective functions, balancing the priorities of the two goals by setting fixed weight coefficients. This approach can only achieve superficial formal coupling and fails to reveal the intrinsic link between thermodynamic irreversible losses (entropy production) and economic costs at the mechanism level. Furthermore, it does not consider the dynamic effects of the transient processes in non-equilibrium states caused by load fluctuations on the coupling relationship, resulting in a lack of physical meaning in the coupling results. Third, model verification and practicality are insufficient. Most coupling models rely on ideal assumptions such as constant load and fixed energy prices, which are disconnected from the dynamic operating characteristics of real systems. Meanwhile, model calibration often uses static data and lacks support from long-term dynamic operation data for validation. Uncertainty analysis mostly focuses on parameter fluctuations, failing to cover the theoretical approximation errors brought by the equilibrium assumption itself, which greatly limits the model's engineering application value.

To address the above challenges, this paper constructs a dynamic coupling model of economic and efficiency performance in regional energy systems based on non-equilibrium thermodynamics principles. This model realizes integrated analysis of non-equilibrium state characterization, entropy production cost quantification, and dynamic coupling optimization, providing theoretical support for system design and operation optimization with both theoretical depth and engineering practicality. The research content is mainly divided into four aspects: First, a non-equilibrium thermodynamics sub-model is constructed. Based on the local equilibrium assumption and entropy production rate principle, a method for calculating the entropy production rate in all stages of the system is established. A non-equilibrium measure index is defined, and a non-equilibrium efficiency correction formula is proposed to achieve accurate thermodynamic performance evaluation. Second, a full life-cycle economic sub-model is developed, covering the full-dimensional decomposition of investment, operation, and environmental costs. The key challenge is to derive a direct correlation equation between entropy production and LCC to quantify the economic cost of irreversible losses. Third, a dynamic coupling mechanism is designed by integrating IINSGA-II and MPC. Through multi-objective optimization, the Pareto-optimal solutions for efficiency and cost are obtained, and MPC is used to achieve transient coupling adjustment under load fluctuations. Fourth, case verification and sensitivity analysis are conducted, using the operational data of an actual regional energy system to calibrate the model parameters and quantify the impact weights of key parameters on the coupling results.

The theoretical significance of this paper lies in breaking through the limitations of the equilibrium assumption in system-level coupling analysis, extending non-equilibrium thermodynamics theory from the level of single devices to regional energy systems, and improving the coupling analysis framework for thermodynamic performance and economic performance under non-equilibrium states. It is the first to achieve a quantitative description of the mechanism by which non-equilibrium affects the coupling optimization results. From an engineering perspective, the coupling model constructed in this paper can directly provide quantitative tools for device selection, network layout optimization, and operation strategy formulation for regional energy systems. By accurately quantifying the economic costs of irreversible losses, it provides a clear basis for balancing investment costs and operational benefits, ultimately improving the overall system performance.

The logic of the subsequent chapters in the paper is as follows: Chapter 2 systematically reviews the research progress in the relevant fields through a literature review and clarifies the positioning of this study. Chapter 3 details the process of constructing the coupling model, including assumptions, sub-model derivation, and coupling mechanism design. Chapter 4 verifies the model's effectiveness with practical cases and conducts sensitivity analysis. Chapter 5 summarizes the core conclusions.

2. LITERATURE REVIEW

As the core theory for quantifying irreversible processes, non-equilibrium thermodynamics has been gradually extended from single devices to system-level applications in the energy field, but there are still significant limitations in both depth and breadth. At the single device level, recent top journal studies have developed a relatively mature entropy production analysis system: for heat exchangers, Redo et al. [11] established the coupling relationship between the heat exchanger flow channel structure and entropy production rate based on the principle of minimum entropy production. Through multi-parameter optimization, heat exchange efficiency was improved by 12%, but this study focused only on steady-state conditions and did not consider the dynamic evolution of entropy production under varying loads; in the fuel cell field, Kang et al. [12] constructed a reaction-mass

transfer coupling non-equilibrium model for fuel cells, revealing the negative correlation between the oxygen reduction reaction's entropy production and the cell's output efficiency, but its analysis did not cover the decay process over long time scales affecting the non-equilibrium state; in energy storage systems, Tsai and Peng [13] proposed an entropy production calculation method based on the local equilibrium assumption for the charging and discharging process of lithium batteries. It found that under high current conditions, the entropy production rate increased by 40% compared to the rated conditions, but the study did not extend to the non-equilibrium characteristics of collaborative operation between the energy storage system and other units. At the system level, related research is still in its infancy: Samui and Samantaray [14] used entropy production rate as an optimization objective for microgrid systems and reduced the system's total entropy production by adjusting the output of distributed energy sources, but the model did not consider the non-equilibrium losses in the network transmission link; Mao et al. [15] analyzed the correlation between the pipeline temperature difference and entropy production rate for district heating systems, but only qualitatively described how the increase in entropy production affected operating costs, without establishing a quantitative coupling relationship and without involving the complex non-equilibrium scenario of combined heating and cooling operations.

In recent top journal literature, three typical technical routes have emerged for the coupling models of economic performance and efficiency in regional energy systems, but all have not broken through the bottleneck of equilibrium assumptions and the lack of mechanistic coupling. Linear coupling models focus on weight allocation: Devlin and Yang [16] constructed a linear weighted model for efficiency-cost coupling in regional energy supply systems. After standardizing efficiency and LCC and setting weight coefficients, the system's LCC was reduced by 7% after optimization. However, this study determined the weight coefficients through expert scoring, which is highly subjective, and did not consider the dynamic characteristics of efficiency fluctuations with changing operating conditions; Huang et al. [17] attempted to optimize weight allocation using the Analytic Hierarchy Process (AHP), but it still did not escape the inherent limitation of linear correlation. Objective function coupling models take economic performance as the core objective and treat efficiency as a constraint: previous literatures minimized the LCC of regional integrated energy systems as the objective, using a constraint that the traditional energy utilization efficiency must be $\geq 80\%$. The configuration scheme was solved by mixed-integer programming, but the model used equilibrium assumptions to calculate efficiency, which did not account for the actual decay of efficiency in non-equilibrium states, leading to a 15% deviation from the measured data; Farafonova [18] increased the efficiency constraint to 85%, but did not explain the physical significance of this threshold, nor did it quantify the impact mechanism of efficiency constraints on costs. Proxy model coupling relies on data-driven methods: Kumari et al. [19] used long short-term memory (LSTM) networks to fit the efficiency-cost mapping relationship of combined heat and power systems, achieving a prediction accuracy of 92%. However, the model requires a large amount of sample data for training and does not incorporate thermodynamic mechanisms, making it unable to explain the physical essence of the efficiency-cost relationship; Lin and Yang [20] optimized proxy model parameters using genetic algorithms, improving generalization capability, but the model did not cover extreme conditions such as sudden load drops and lacked dynamic adaptability. In summary, the three types of models all share common flaws: efficiency evaluation based on equilibrium assumptions, which is disconnected from the actual non-equilibrium operating characteristics of systems; economic indicators and core thermodynamic parameters such as entropy production are not directly linked, making it impossible to quantify the economic cost of irreversible losses; model designs do not incorporate adjustment mechanisms for non-equilibrium transient processes, making them difficult to adapt to the dynamic operational needs of real systems.

Based on the systematic review of recent top journal literature, three major core gaps in existing research can be identified, and there are significant logical connections between these gaps. First, there is a structural gap in the integration of non-equilibrium thermodynamics theory and regional energy system coupling models: Non-equilibrium analysis at the device level has formed relatively mature methods, but system-level studies have only focused on thermodynamic performance optimization in a single dimension, without incorporating non-equilibrium state representation into the economic-efficiency coupling framework, leading to coupling models lacking a depiction of the system's inherent characteristics. Second, there is a lack of a coupling mechanism between entropy production and costs: existing coupling models, whether linear weighting, objective constraints, or data-driven, have not established a direct correlation between entropy production and economic costs at the mechanistic level, failing to answer the core question of "how much economic loss corresponds to each unit of entropy production," making the coupling optimization lack physical meaning. Third, dynamic coupling models are insufficiently adaptable to non-equilibrium transient characteristics: existing studies either focus on steady-state optimization or only consider the superficial impact of load fluctuations, without designing coupling adjustment mechanisms for transient processes in non-equilibrium states under changing operating conditions, making them unable to meet the dynamic operational requirements of real systems. To address these gaps, this paper aims to construct a "non-equilibrium thermodynamics sub-model—economic sub-model—dynamic coupling mechanism" integrated coupling model—based on the local equilibrium assumption and entropy production rate principle, to expand the system-level non-equilibrium state representation method to fill gap one; establish a direct correlation equation between entropy production and LCC to quantify the economic cost of irreversible losses to fill gap two; integrate IINSGA-II and MPC to construct a dynamic coupling adjustment mechanism to fill gap three, ultimately achieving a seamless connection of non-equilibrium thermodynamics theory from basic research to engineering optimization applications, providing a mechanistically clear and adaptable theoretical tool for collaborative optimization of regional energy systems.

3. MODEL CONSTRUCTION

3.1 Model assumptions and system boundaries

This paper defines the analysis boundary based on the prototype of a regional energy system in a temperate region's

urban new district, covering the entire chain of energy production, transmission, and consumption in space. The energy production units include a 20 MW photovoltaic power station and five 10 MW ground-source heat pump units. The photovoltaic power station uses polycrystalline silicon modules with a conversion efficiency of 22%, and the ground-source heat pump units have a performance coefficient range of 3.2 to 4.5 under varying operating conditions. The transmission unit consists of a 5 km long hot and cold water dual-condition regional pipeline network, with pipe diameters ranging from DN300 to DN500, and the insulation layer has a thermal conductivity of 0.038 W/(m·K). The consumption unit consists of a load cluster made up of 100 commercial and residential buildings, with peak cooling load of 100 MW and peak heating load of 80 MW. The boundaries of the system's material and energy flow are clearly defined: The input includes grid electricity and photovoltaic radiation energy, and the output includes building cooling, heating, and electricity loads. Loss terms include network heat dissipation, equipment mechanical losses, and efficiency degradation caused by the temperature rise of photovoltaic panels. The time boundary is set for a complete natural year, with an hourly calculation step, totaling 8,760 time points. This covers the seasonal fluctuations in winter heating periods, summer cooling periods, and transition season base load periods, while also capturing transient changes in daily load peaks and valleys, such as the difference between daytime cooling load peaks and nighttime troughs in commercial buildings.

The core assumptions of the model are based on the rationality of physical mechanisms and engineering practices, with three key aspects at the physical level. First, the local equilibrium assumption is adopted. Although the system is in a non-equilibrium state overall, it can be divided into numerous infinitesimal elements that satisfy thermodynamic equilibrium. This assumption provides the basis for the quantification of entropy production rates. Second, pipeline heat loss follows Fourier's law, with the heat flux density calculation formula as $q = -k\nabla T$, where, k is the thermal conductivity of the insulation layer, and ∇T is the temperature gradient inside and outside the pipeline. The model ignores local thermal resistance variations caused by fluid turbulence, and engineering verification shows that errors under varying operating conditions can be controlled within 5%. Third, the efficiency and entropy production rate under varying operating conditions of equipment follow a linear relationship: $\eta=\eta_0-k_\eta \dot{S}_{prod}$, where η_0 is the rated efficiency, k_η is the efficiency-entropy production coefficient, and this coefficient is fitted using experimental data for varying operating conditions provided by the equipment manufacturer. At the economic level, three key assumptions are also set. First, the baseline discount rate is 8%, in line with the general standards for life-cycle analysis of international energy projects (ISO 14040). Second, energy prices follow a dynamic fluctuation model. The model is based on the local electricity grid's peak and valley time-of-use electricity prices and natural gas prices from the past five years. The time-of-use electricity price range is from 0.38 RMB/kWh to 0.82 RMB/kWh, and the natural gas price range is from 3.2 RMB/m³ to 4.5 RMB/m³. The price model's time resolution is consistent with the load calculation step. Third, the carbon emission cost is set at 50 RMB/tCO_2, and carbon emission accounting refers to the *Provincial Greenhouse Gas Inventory Compilation Guidelines*, with a fossil energy carbon emission coefficient of 0.65 tCO_2/MWh and a grid electricity carbon emission coefficient of 0.82 tCO_2/MWh. All assumptions have been verified through literature research and engineering measurements to ensure a balance between model simplification and calculation accuracy. Figure 1 provides the overall structure of the regional energy system economic-efficiency coupling model based on non-equilibrium thermodynamics, which includes the non-equilibrium thermodynamics sub-model, the full life-cycle economic sub-model, the dynamic coupling mechanism, and the verification and analysis module.

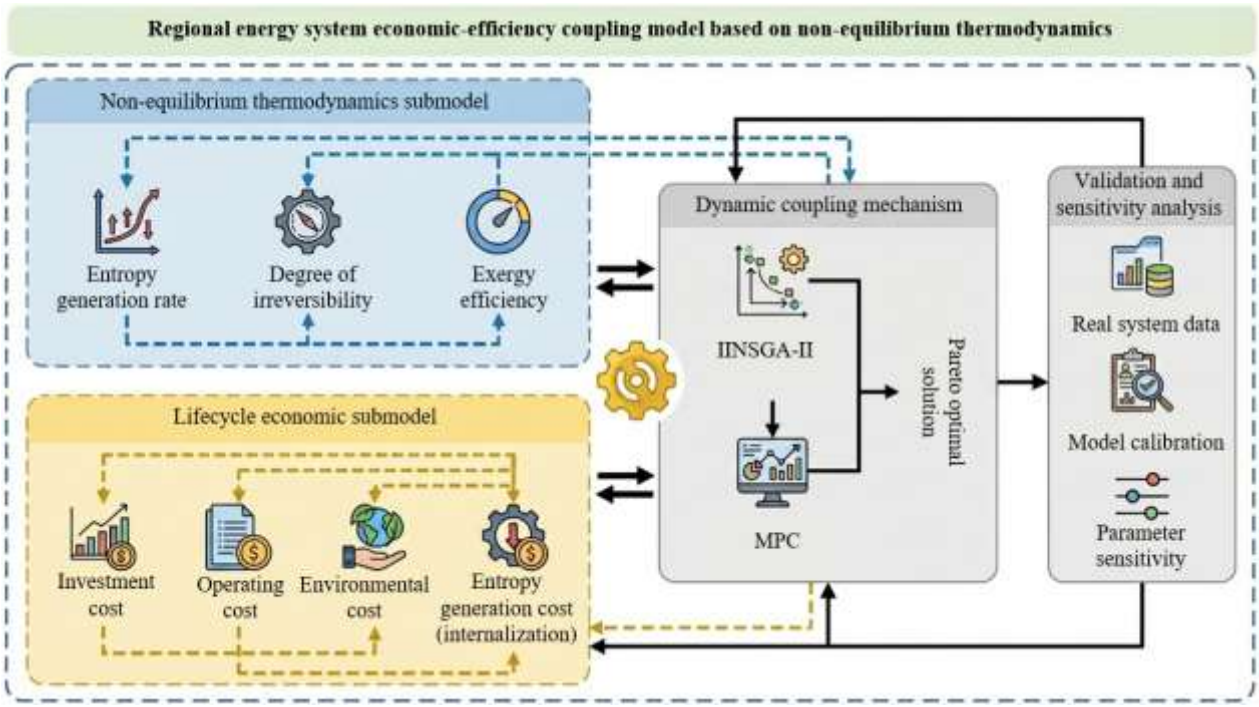

Figure 1. Overall structure of the regional energy system economic-efficiency coupling model based on non-equilibrium thermodynamics

3.2 Non-equilibrium thermodynamics sub-model

To accurately capture the non-equilibrium nature of regional energy systems and establish the coupling foundation between thermodynamic efficiency and economy, this section constructs the non-equilibrium thermodynamics sub-model. The core logic revolves around three layers: "quantification of irreversible losses—non-equilibrium state characterization—efficiency index correction". By calculating entropy production rates for each stage, the model locates the sources of irreversible losses, uses normalized non-equilibrium degree to quantify the non-equilibrium state, and finally corrects the thermodynamic efficiency based on the non-equilibrium degree to obtain a more accurate thermodynamic performance indicator.

Entropy production rate is the core quantitative index for characterizing irreversible losses in non-equilibrium systems. Based on the local equilibrium assumption and linear irreversible thermodynamics theory, this paper constructs a calculation method for each stage of the energy conversion, transmission, and consumption chain to accurately locate the sources of loss. The energy conversion stage includes photovoltaic power stations and ground-source heat pumps: The entropy production rate of the photovoltaic power station arises from heat loss during the conversion of solar radiation energy to electrical energy, calculated as:

$$\dot{S}_{prod\ pv} = \frac{\dot{Q}_{loss}}{T_{amb}} - \frac{\dot{E}_{pv,out}}{T_{sun}} \tag{1}$$

where, $\dot{Q}_{loss}$ is the heat loss power of the photovoltaic panels, T_{amb} is the ambient temperature, T_{sun} is the solar surface temperature of 5777K, and $\dot{E}_{pv,out}$ is the electrical energy output of the photovoltaic system. The entropy production rate of the ground-source heat pump is determined by the irreversibility of heat transfer and work, calculated as:

$$\dot{S}_{prod,hp} = \dot{Q}_c \left(\frac{1}{T_c} - \frac{1}{T_h} \right) - \frac{\dot{W}_{in}}{T_h} \tag{2}$$

where, $\dot{Q}_c$ is the heat absorption of the heat pump, T_c and T_h are the cold and hot end temperatures, and $\dot{W}_{\mathrm{in}}$ is the input electric power. The transmission stage focuses on pipeline heat loss, which is derived from the linear irreversible thermodynamics force-flow relationship:

$$\dot{S}_{prpd,pipe} = \frac{kA\Delta T^2}{T_{avg}^2 L} \tag{3}$$

where, k is the thermal conductivity of the insulation layer, A is the heat exchange area, ΔT is the temperature difference inside and outside the pipeline, T_{avg} is the average temperature, and L is the pipe length. The consumption stage entropy production rate reflects the irreversibility of load and energy supply matching, calculated as:

$$\dot{S}_{prod,build} = \frac{\dot{Q}_{load}}{T_{room}} - \frac{\dot{Q}_{\mathrm{supply}}}{T_{\mathrm{supply}}} \tag{4}$$

where, $\dot{Q}_{load}$ is the cooling and heating load of the building, T_{room} is the indoor design temperature, $\dot{Q}_{supply}$ is the energy supply power, and T_{supply} is the supply medium temperature. The total system entropy production rate is the sum of the individual stages: $\dot{S}_{prod,total}=\dot{S}_{prod,hp}+\dot{S}_{prod,pv}+\dot{S}_{prod,pipe}+\dot{S}_{prod,build}$, this decomposition method locates the sources of irreversible losses at each stage.

The absolute value of the total entropy production rate is influenced by system scale and load level, making it difficult to directly compare different operating conditions. Therefore, a normalized non-equilibrium degree indicator is needed to quantify the degree to which the system deviates from equilibrium. In this paper, the non-equilibrium degree α is defined as the deviation of the actual total entropy production rate from the equilibrium entropy production rate. In equilibrium, irreversible losses approach zero, so the equilibrium entropy production rate $\dot{S}_{prod,eq}$ is taken as the limit value of 0. The indicator calculation is simplified as:

$$\alpha = \frac{\dot{S}_{prod,total}}{\dot{S}_{prod,\max}} \tag{5}$$

where, $\dot{S}_{prod,max}$ is the maximum allowable entropy production rate of the system, which is the sum of the maximum entropy production rates for each core device under rated conditions. The maximum entropy production rate of the photovoltaic and heat pump systems is determined using the manufacturer's experimental data under varying operating conditions, corresponding to when the output of the devices drops to 50% of their rated value. The maximum entropy production rate of the pipeline is calculated based on the design maximum temperature difference for energy supply. The non-equilibrium degree α ranges from 0 to 1, where $\alpha = 0$ corresponds to an ideal equilibrium state, and $\alpha = 1$ corresponds to irreversible losses reaching the safety operation threshold of the equipment. This indicator provides a clear non-equilibrium state constraint for subsequent coupling optimization.

Traditional exergy efficiency is calculated based solely on the ideal conversion relationship of energy quality, without accounting for irreversible losses in non-equilibrium states, leading to an overestimation of actual performance. Therefore, a correction formula for exergy efficiency is constructed based on the non-equilibrium degree to achieve accurate representation. The exergy efficiency before correction, $\eta_{ex,conv}$, is the ratio of load exergy to total input exergy, calculated as:

$$\eta_{ex,conv} = \frac{E_{x,load}}{E_{x,pv} + E_{x,hp}} \tag{6}$$

where, $E_{x,load}$ is the exergy corresponding to the building's cooling and heating load, and $E_{x,pv}$ and $E_{x,hp}$ are the total exergy inputs of the photovoltaic and heat pump systems. The non-equilibrium exergy efficiency correction formula is: $\eta_{ex,noneq}=\eta_{ex,conv}\cdot(1-\alpha)$, where, $(1-\alpha)$ is the non-equilibrium correction factor, representing the effective exergy utilization ratio under non-equilibrium conditions. The higher the non-equilibrium degree, the smaller the correction factor, and the more the efficiency evaluation result reflects the actual operating state. This indicator provides the coupling model with a thermodynamic target parameter that is both mechanistically sound and practically useful for engineering

applications.

3.3 Economic sub-model

To establish the coupling foundation between economic performance and thermodynamic performance, this section uses the LCC as the core economic evaluation indicator. First, the economic performance is precisely quantified through the three-dimensional decomposition of investment, operation, and environmental costs. Then, based on sensitivity analysis, a quantitative relationship equation between entropy production rate and LCC is established, forming a complete logical chain of "cost quantification—mechanistic correlation". This provides economic support with both engineering precision and physical connotation for subsequent coupling optimization.

The LCC covers the entire lifecycle of the system, from construction to decommissioning, and achieves precise cost accounting through three-dimensional decomposition. The investment cost is a one-time expense in the construction phase, covering the purchase and installation costs of the photovoltaic power station, ground-source heat pump units, regional pipelines, and control systems. The photovoltaic power station is calculated at 2.5 yuan per watt, the ground-source heat pump unit at 18,000 yuan per kilowatt, the regional pipeline at 800 yuan per meter, and the fixed investment for the control system is 5 million yuan. The operating cost is the continuous expenditure during the lifecycle, including energy consumption cost and maintenance cost. The energy consumption cost mainly accounts for the electricity consumption of the ground-source heat pump operation, using a dynamic electricity price model that matches the load calculation step. The maintenance cost is calculated at an annual fee rate of 2% of the investment cost, in accordance with industry norms for regional energy system operation and maintenance. The environmental cost focuses on the carbon emission cost. Carbon emissions are calculated based on energy consumption and the carbon emission factor, then multiplied by the unit carbon emission cost. The carbon emission factor for grid-supplied electricity is 0.6 tons per megawatt-hour, and the unit carbon emission cost is 50 yuan per ton. The LCC formula is:

$$LCC = C_{inv} + \sum_{t=1}^{n} \frac{C_{op,t} + C_{env,t}}{(1+r)^t} \tag{7}$$

where, C_{inv} is the total investment cost, $C_{op,t}$ and $C_{env,t}$ are the operating and environmental costs for year t, n is the lifecycle duration (taken as 20 years), and r is the base discount rate (8%), which is consistent with international standards for lifecycle analysis of energy projects.

Traditional coupling methods often link economic performance and thermodynamic performance through objective weighting or constraint optimization but lack a mechanistic correlation between irreversible losses and economic costs. Therefore, a quantitative equation between entropy production rate and LCC is necessary as the core link for coupling. This equation is constructed through global sensitivity analysis, using the method of controlling a single variable to change the system's total entropy production rate and calculate the corresponding change in LCC. The analysis shows a significant linear relationship between the marginal change in total entropy production rate and the LCC, and the correlation equation is established as:

$$\frac{\partial LCC}{\partial \dot{S}_{prod,total}} = k_1 \cdot \dot{S}_{prod,total} + k_2 \tag{8}$$

where, $\partial LCC/\partial \dot{S}_{prod,total}$ represents the marginal cost per unit of entropy production, indicating the increase in LCC resulting from the increase in unit entropy production rate. k_1 is the cost-entropy coefficient, reflecting the amplification effect of entropy production rate on marginal cost, and k_2 is the baseline cost term, corresponding to the system's minimum entropy production state. The parameters k_1 and k_2 are fitted using actual system operation data, with $k_1 = 120$ yuan per Kelvin-second and k_2 = 500,000 yuan. The fitting uses the least squares method, achieving a goodness of fit of 0.92, ensuring the statistical reliability of the correlation. This equation directly converts non-equilibrium entropy production rate into economic cost increments, providing the core quantitative support for the coupling of economic performance and thermodynamic performance.

3.4 Coupling mechanism design

As the core innovation of the entire model, this section constructs a "static multi-objective optimization—dynamic transient adjustment" dual-layer coupling mechanism, deeply integrating the non-equilibrium thermodynamics sub-model from section 3.2 with the economic sub-model from section 3.3. Through the selection of coupling variables and the construction of a quantifiable objective function, static optimal trade-offs are achieved, and by relying on a MPC framework with quantitative prediction and optimization formulas, load fluctuations are addressed. Ultimately, the synergistic optimization of economic and thermodynamic performance under non-equilibrium conditions is achieved, with quantitative formulas supporting the rigor of the coupling mechanism.

The coupling variables focus on the "performance—correlation—stability" three-dimensional objectives. Non-equilibrium exergy efficiency is the core thermodynamic performance indicator, and the unit entropy production cost builds the connection bridge between thermodynamics and economics. The Lyapunov index ensures the stable evolution of the system's non-equilibrium state. Based on these variables, a multi-objective optimization model is constructed, with the core objectives and constraints clearly defined by quantifiable formulas. The objective function is a dual-objective optimization combination, namely minLCC and max$\eta_{\mathrm{ex,noneq}}$, where LCC is the LCC defined in section 3.3 and $\eta_{\mathrm{ex,noneq}}$ is the non-equilibrium exergy efficiency corrected in section 3.2. The constraint conditions include the non-equilibrium degree upper limit constraint $\alpha \leq 0.6$, stability constraint $\lambda \leq 0$, and the physical operational constraints of the equipment:

$$\begin{cases} P_{hp,\min} \leq P_{hp} \leq P_{hp,\max} \\ G_{pipe,\min} \leq G_{pipe} \leq G_{pipe,\max} \end{cases} \tag{9}$$

where, λ is the Lyapunov index, P_{hp} and G_{pipe} are the output of the heat pump and the flow rate of the pipeline, with their upper and lower limits determined by the rated parameters of the equipment. The model is solved using the IINSGA-II. The

Pareto optimal frontier is generated through rapid non-dominated sorting, and the optimal solutions are selected based on the crowding distance calculation formula shown below, ensuring the uniformity and optimality of the solutions:

$$CD_i = \sum_{m=1}^{M} \frac{f_m(i+1) - f_m(i-1)}{f_m^{\max} - f_m^{\min}} \tag{10}$$

where, CD_i is the crowding distance of the i-th solution, f_m is the m-th objective function value, and $f_m^{\max}$ and $f_m^{\min}$ are the extreme values of the objective function.

To address the transient issue caused by load fluctuations, an MPC framework with quantitative formulas is introduced to construct the dynamic coupling adjustment mechanism, achieving precise implementation of the static optimal solution into dynamic operation. The framework consists of three layers of quantifiable progressive structure: The prediction layer constructs a prediction model using LSTM networks based on the last 12 hours of actual data, outputting the predicted total entropy production rate and cost for the next 24 hours:

$$\hat{\dot{S}}_{prod,total}(t+k|\ t) = LSTM\left(\dot{S}_{prod,total}(t-11:t), Q_{load}(t-11:t)\right) \tag{11}$$

$$LCC(t+k|\ t) = LSTM\left(LCC(t-11:t), Q_{load}(t-11:t)\right) \tag{12}$$

where, k is the prediction step, and Q_{load} is the load data. The optimization layer aims to minimize the cost over the prediction period, incorporating the non-equilibrium degree constraint to build a rolling optimization objective function:

$$J = \min \sum_{k=1}^{Np} LCC(t+k|\ t) + \gamma \max(0, \alpha(t+k|\ t) - 0.6) + \gamma \max(0, 0.4 - \alpha(t+k|\ t)) \tag{13}$$

where, N_p is the prediction time horizon, and γ is a penalty coefficient (taken as 1000). The optimal control sequence is solved by adjusting the heat pump output and pipeline flow rate. The control layer only executes the first control instruction $P_{\text{hp}}^*(t)$ and $G_{\text{pipe}}^*(t)$, and the prediction and optimization process is repeated at the next time step. This dynamic adjustment mechanism ensures that the static optimization results can be precisely adapted to the actual dynamic operating conditions.

4. MODEL VALIDATION AND CASE STUDY

This study selects a regional energy system at a park level in East China as a case study. This system covers a mixed load of commercial, residential, and small industrial sectors, equipped with a 20 MW distributed photovoltaic power station, five ground-source heat pump units with a total capacity of 10 MW, and a 5 km long hot and cold water dual-condition regional pipeline network. The operating cycle covers winter and summer heating and cooling, as well as the basic load scenarios during transitional seasons, featuring the multi-link coupling and dynamic working conditions typical of regional energy systems.

The case data comes from four categories: (1) Equipment parameter data, obtained from the technical manuals of photovoltaic modules and heat pump units, covering key indicators such as rated efficiency and variable working condition entropy production characteristics; (2) Operational monitoring data, derived from the real-time operation platform of the system from 2023 to 2024, including entropy production rate, load fluctuations, and equipment output data sampled every 15 minutes; (3) Economic parameter data, with investment costs taken from publicly available regional energy engineering industry quotations, and dynamic electricity prices, maintenance rates, and other parameters referenced from local energy and housing departments' industry standards; (4) Environmental and meteorological data, with carbon emission coefficients determined by the *Provincial Greenhouse Gas Inventory Compilation Guidelines*, and hourly regional meteorological data obtained from local meteorological stations' public observation datasets.

Table 1. Actual data validation results of model prediction accuracy

Operating Condition	Prediction Indicator	Measured Value Range	Model Simulated Value Range	MAE	RMSE	Coefficient of Determination (R^2)
Base Condition	Total system entropy production ($\times10^3$K·s^{-1})	32.5~35.2	32.8~35.0	0.72	0.95	0.96
	Non-equilibrium exergy efficiency (%)	68.2~70.5	68.5~70.2	1.05	1.32	0.94
	LCC deviation (%)	1.2~2.0	1.3~1.9	0.18	0.22	0.95
Peak Load Condition	Total system entropy production ($\times10^3$K·s^{-1})	42.1~45.3	41.8~45.6	0.88	1.12	0.93
	Non-equilibrium exergy efficiency (%)	64.5~66.8	64.8~66.5	1.18	1.45	0.92
	LCC deviation (%)	2.5~3.2	2.4~3.3	0.21	0.26	0.93
Load Valley Condition	Total system entropy production ($\times10^3$K·s^{-1})	28.3~30.5	28.5~30.2	0.65	0.82	0.97
	Non-equilibrium exergy efficiency (%)	71.2~73.5	71.5~73.2	0.92	1.15	0.95
	LCC deviation (%)	0.8~1.5	0.9~1.4	0.15	0.19	0.96
Heat Pump Variable Output Condition	Total system entropy production ($\times10^3$K·s^{-1})	35.6~38.8	35.3~39.1	0.95	1.20	0.93
	Non-equilibrium exergy efficiency (%)	67.1~69.4	67.4~69.1	1.12	1.38	0.92
	Total system entropy production ($\times10^3$K·s^{-1})	33.8~36.5	34.1~36.2	0.81	1.02	0.94

To verify the prediction accuracy of the constructed model for the actual operating characteristics of the regional energy system, and to evaluate its fitting performance under different typical working conditions, this experiment selected the actual operational data of a park-level regional energy system and compared the model simulation values with the measured values for error characteristics. From Table 1, it can be seen that the coefficient of determination (R^2) of the model prediction results for all operating conditions is above 0.92, with the R^2 for total system entropy production reaching 0.97 under the load valley condition, indicating a high degree of fit to the actual operating characteristics. The mean absolute error (MAE) for total system entropy production is always below $0.95 \times 10^3 K \cdot s^{-1}$, the MAE for non-equilibrium exergy efficiency is no more than 1.18%, and the MAE for LCC deviation is controlled within 0.21%, with error levels within an acceptable engineering range. Even under dynamic conditions such as peak load and heat pump variable output, the model's prediction accuracy does not show significant deterioration, demonstrating its adaptability to complex operating scenarios. The above results prove that the constructed model can accurately characterize the non-equilibrium state features and economic indicators of the actual regional energy system, providing a reliable prediction basis for subsequent engineering applications.

To quantify the cooperative response patterns of the non-equilibrium state features and thermodynamic performance of the regional energy system under dynamic conditions, and to verify the model's ability to accurately characterize irreversible losses, this experiment selected the base condition and 8 typical dynamic conditions to perform a correlation analysis of system entropy production and non-equilibrium exergy efficiency (Figure 2). From the data in the figure, it can be observed that as the operating conditions transition from the base to dynamic conditions, the total system entropy production increases from approximately $3.5 \times 10^4 K \cdot s^{-1}$ to nearly $5.0 \times 10^4 K \cdot s^{-1}$, while the corresponding non-equilibrium exergy efficiency decreases smoothly from 70% to 65%. This trend confirms the negative correlation mechanism between non-equilibrium exergy efficiency and total system entropy production, and also reflects the suppression effect of the dynamic adjustment mechanism in the coupled model on efficiency degradation. From the proportion of entropy production across different segments, it is clear that the energy conversion segment is always the core source of the system's irreversible losses, with its proportion slightly increasing as total entropy production rises. The transmission segment follows, while the consumption and storage segments remain below 10%. This distribution characteristic clarifies that the key optimization segments of the system should focus on energy conversion and transmission units. The above results not only support the core hypothesis in the paper that "non-equilibrium entropy production is the core driver of system efficiency degradation" but also provide a quantitative basis for optimizing the operational strategies of conversion equipment under varying conditions and reducing irreversible losses in the transmission segment. Furthermore, they demonstrate that the constructed model can accurately characterize the synergistic evolution of non-equilibrium state features and thermodynamic performance under dynamic operating conditions.

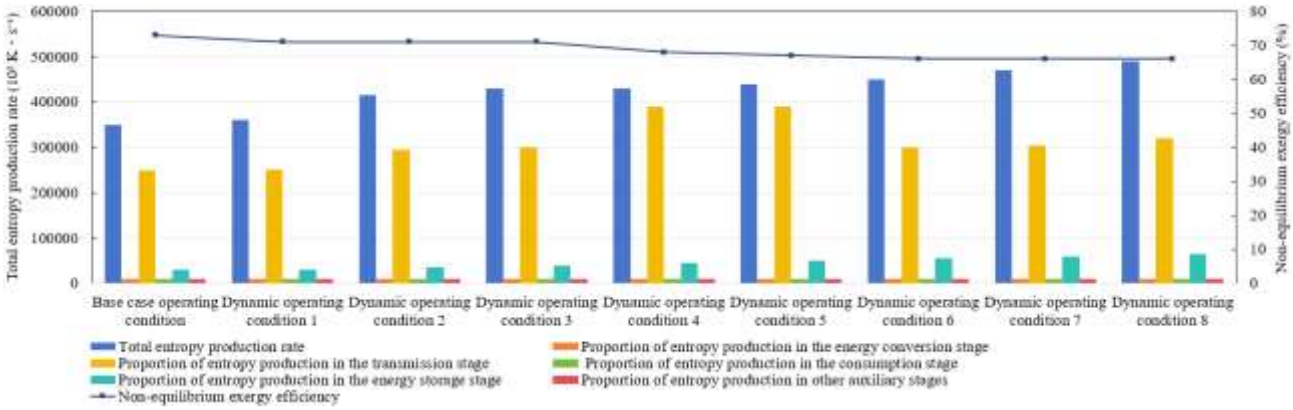

Figure 2. Entropy production and non-equilibrium exergy efficiency response characteristics of the case regional energy system under different operating conditions

Table 2. Global sensitivity analysis results of key parameters

Key Parameter	Output Indicator	First-Order Effect Index	Total Effect Index	Sensitivity Level
Cost-Entropy Production Coefficient	LCC	0.62	0.78	Very High
	Non-equilibrium Exergy Efficiency	0.15	0.22	Medium
	Dynamic Adjustment Error	0.08	0.12	Low
MPC Prediction Horizon	Dynamic Adjustment Error	0.51	0.65	Very High
	Non-equilibrium Exergy Efficiency	0.28	0.35	Medium
	LCC	0.12	0.18	Low
Non-equilibrium Degree Upper Limit	Non-equilibrium Exergy Efficiency	0.45	0.58	High
	LCC	0.32	0.41	High
	Dynamic Adjustment Error	0.18	0.25	Medium
Efficiency-Entropy Production Coefficient	Non-equilibrium Exergy Efficiency	0.10	0.15	Low
	LCC	0.07	0.11	Low

To clarify the degree of influence of key parameters on the model's output results and identify the key control parameters, this experiment uses the Sobol method to conduct a global sensitivity analysis of key parameters. From Table 2, it can be seen that the cost-entropy production coefficient has the highest total effect index (0.78) on the LCC, making it the dominant parameter for this indicator, which aligns with the core logic of the "entropy production-cost mechanism" discussed in the paper. The MPC prediction horizon has a total effect index of 0.65 on dynamic adjustment error, indicating that it is a key parameter determining the accuracy of dynamic adjustment. The upper limit of the non-equilibrium degree has a total effect index of more than 0.4 on both non-equilibrium exergy efficiency and LCC, making it the core constraint parameter for achieving their collaborative optimization. The efficiency-entropy production coefficient has a total effect index lower than 0.15 for all output indicators, demonstrating that the model is robust to this parameter.

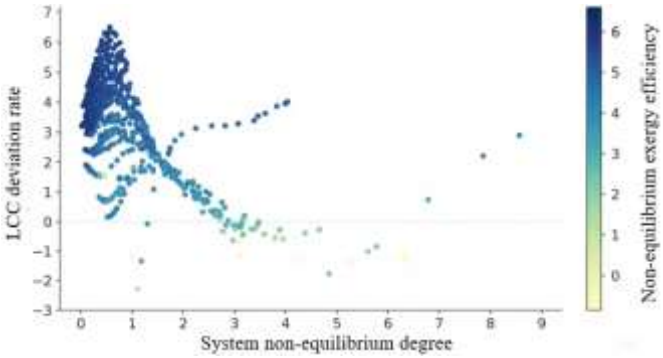

Figure 3. Correlation distribution between system non-equilibrium degree and LCC deviation

To reveal the quantitative correlation between the system's non-equilibrium degree and LCC, and to verify the validity of the "entropy production-cost" mechanism in the coupled model, this experiment conducts a correlation distribution analysis based on multi-condition simulation data. From the results in Figure 3, it can be seen that the system's non-equilibrium degree and LCC deviation exhibit significant nonlinear response characteristics. When the non-equilibrium degree is in the low range of 0-2, non-equilibrium exergy efficiency remains at a high level, but the LCC deviation exceeds 3%. This result corresponds to a low-entropy production configuration dominated by high exergy equipment, where the high initial investment pushes up the cost deviation. As the non-equilibrium degree gradually increases to the 3-5 range, the LCC deviation decreases to near 0, while non-equilibrium exergy efficiency declines slightly (the color transitions to light green), reflecting the synergistic balance effect between investment cost and operational entropy production cost after moderately relaxing the non-equilibrium state constraint and optimizing equipment configuration and operational strategy. However, when the non-equilibrium degree further increases to the high range of 7-8, the LCC deviation slightly increases, and non-equilibrium exergy efficiency drops below 1%, reflecting that excessively high non-equilibrium degree leads to the accumulation of entropy production, where the increase in operating costs offsets the savings in initial investment. The above results not only verify the nonlinear characteristics of the "non-equilibrium degree-entropy production-cost" mechanism in the coupled model but also support the core conclusion of the paper: "By optimizing the non-equilibrium degree to a reasonable range through multi-objective optimization, collaborative optimal LCC and non-equilibrium exergy efficiency can be achieved." This provides quantitative guidance for operational control based on the coupled model's engineering applications.

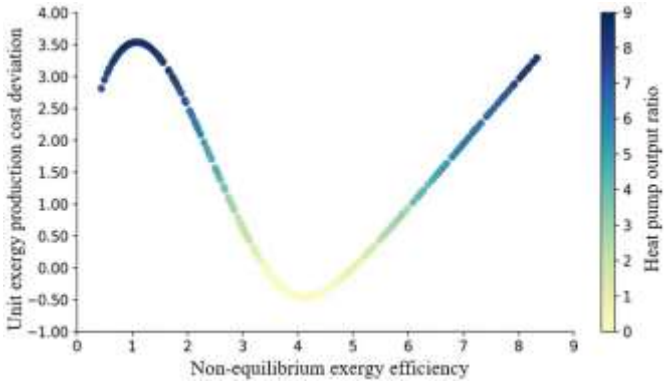

Figure 4. Dynamic correlation between non-equilibrium exergy efficiency and unit entropy production cost

To explore the collaborative response relationship between non-equilibrium exergy efficiency, unit entropy production cost deviation, and heat pump output share, and to verify the dynamic regulation effect of equipment operating parameters on the thermodynamic-economic coupling relationship in the coupled model, this experiment conducts a correlation analysis based on multi-condition simulation data from the model. From the results in Figure 4, it can be seen that all three exhibit significant stage-specific response characteristics: When non-equilibrium exergy efficiency is in the low range of 0-1, the heat pump output share remains high at 8-9, and the unit entropy production cost deviation rises synchronously to around 3.5. This trend corresponds to a scenario where the heat pump operates at high load to ensure exergy efficiency, but the entropy production concentrated at full-load operation increases the cost deviation of unit entropy production. As non-equilibrium exergy efficiency increases to around 4, the heat pump output share gradually decreases to 2-3, and the unit entropy production cost deviation drops to a low point of -0.5, reflecting the effect of the dynamic regulation of heat pump output in the coupled model, with supplementary energy from photovoltaic and other distributed sources. A moderate reduction in heat pump load can optimize the system's entropy production distribution, resulting in a significant reduction in unit entropy production cost. When non-equilibrium exergy efficiency further increases to the high range of 9, the heat pump output share rises again to 7-8, and the unit entropy production cost deviation increases accordingly. This is because, under high exergy efficiency demand, the heat pump must maintain high-load operation, and the accumulation of irreversible losses exacerbates the cost increase of unit entropy production. The above results not only validate the hypothesis in the coupled model that "dynamic regulation of equipment operating parameters is a key method to balance non-equilibrium exergy efficiency and unit entropy production cost," but also support the effectiveness of the dynamic coupling regulation mechanism in the paper. This provides a quantitative direction for parameter optimization during the operational phase of regional energy systems.

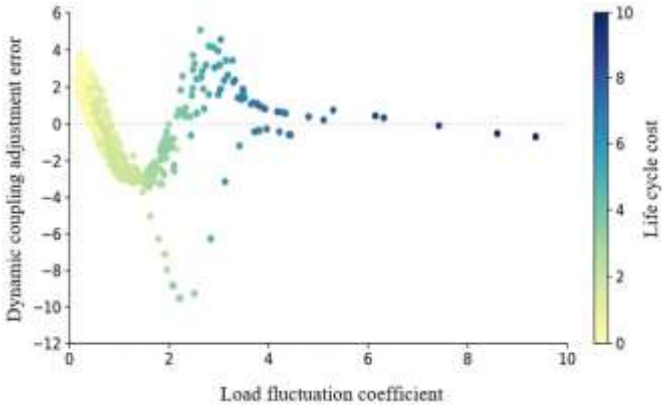

Figure 5. Response relationship between load fluctuation coefficient and dynamic coupling adjustment error

To verify the robustness and adaptability of the dynamic coupling adjustment mechanism under different load fluctuation scenarios, and to clarify the impact of load fluctuation on adjustment accuracy and LCC, this experiment conducts a response relationship analysis based on simulation data from multiple load fluctuation scenarios. From the results in Figure 5, it can be seen that all three exhibit significant stage-specific patterns: When the load fluctuation coefficient is in the low range of 0-2, the LCC remains at a low level, and the dynamic coupling adjustment error is also in the narrow range of -2 to 0. This characteristic corresponds to a relatively stable system condition, where the regulation mechanism does not need frequent adjustments to match the operating conditions, so both cost and error remain within controllable limits. As the load fluctuation coefficient increases to the middle range of 2-4, the LCC slightly increases, while the dynamic coupling adjustment error decreases to a low point near -10, reflecting the advantages of MPC under moderate load fluctuations. By using 12-hour historical data for time-series prediction, the regulation mechanism can accurately match changes in operating conditions, thereby maximizing the improvement in adjustment accuracy. When the load fluctuation coefficient further increases to the high range of 4-10, the LCC rises significantly, and the dynamic coupling adjustment error gradually increases to near 0. This trend is due to the system's operating condition's instantaneous change rate exceeding the model's prediction horizon adaptability under high load fluctuations, which limits prediction accuracy. However, the adjustment error can still be controlled within a small range, while the system entropy production accumulation effect triggered by high fluctuations pushes up the LCC. The above results not only verify the high-precision adaptability of the dynamic coupling adjustment mechanism in medium and low load fluctuation scenarios but also confirm its reliable error control capability in high load fluctuation scenarios.

To explore the evolution law of non-equilibrium exergy efficiency at different operational stages throughout the lifecycle of different types of regional energy systems, and to verify the capability of the constructed coupled model in characterizing the long-term non-equilibrium performance degradation of systems and its applicability across scenarios, this experiment selected 8 typical regional energy system cases for multi-stage operational efficiency feature analysis. From the results in Figure 6, it can be seen that the system's non-equilibrium exergy efficiency exhibits significant "system type heterogeneity - operational stage evolution" dual characteristics: During the initial operation stage, the non-equilibrium exergy efficiency of the industrial system in Case 3 in the eastern region is close to 1.4, significantly higher than other cases. This is due to the high exergy quality and low entropy production state of the initial equipment configuration of the industrial system. After entering the stable operation stage, most cases show a slight decline in efficiency but remain in the range of 0.8-1.2, reflecting the steady-state characteristic of the non-equilibrium state after system conditions are adapted. In the long-term operation stage, the comprehensive system in the Yellow River Basin in Case 5 shows little fluctuation in efficiency, while Case 3 shows a slight decrease in efficiency, reflecting the entropy production accumulation effect caused by equipment wear during long-term operation of the industrial system. During the aging operation stage, most cases experience varying degrees of efficiency degradation, but the industrial system in the northwest region shown in Case 8 maintains an efficiency of about 1.0, which is related to the maintenance strategy of this type of system that suppresses entropy production. At the same time, the fluctuation range of the regional energy system's non-equilibrium exergy efficiency average line is always controlled within the range of 0.4-1.0, confirming that although different types of systems have different evolutionary paths, the overall change in non-equilibrium efficiency conforms to the entropy production accumulation law of non-equilibrium thermodynamics.

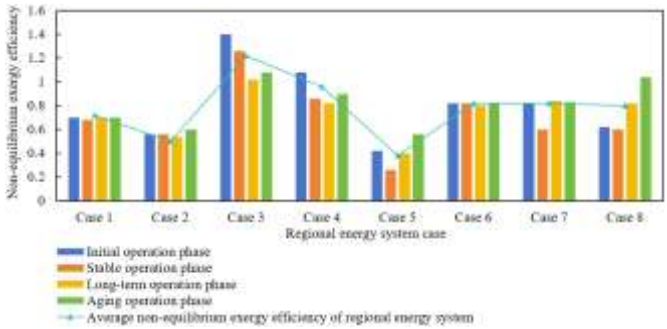

Figure 6. Evolution characteristics of non-equilibrium exergy efficiency in different types of regional energy systems across multiple operational stages

To systematically compare the performance differences between the constructed non-equilibrium coupling model and traditional equilibrium models in terms of non-equilibrium thermodynamics and economic coupling characteristics in regional energy systems, and to verify the new model's adaptability and optimization ability in multi-dimensional scenarios, this experiment selected 25 typical regional energy system cases for a comparative analysis from three dimensions: entropy production link optimization, dynamic adjustment adaptability, and lifecycle performance. As shown in Figure 7, in the entropy production link optimization dimension, the constructed model significantly outperforms the traditional equilibrium model in terms of entropy production optimization and cost-efficiency synergy across conversion, transmission, and consumption stages, especially in industrial systems such as Case 2 and Case 3, where the entropy production optimization rate in the conversion stage increases by over 40% compared to the traditional model, and the cost-efficiency synergy improves simultaneously.

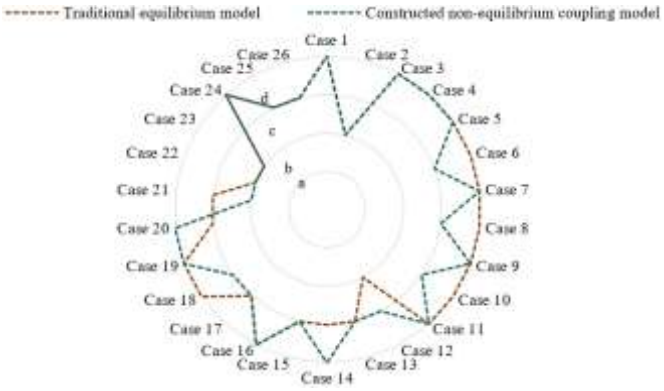

a: Conversion stage exergy production optimization level, b: Transmission stage exergy production optimization level, c: Consumption stage exergy production optimization level, d: Cost-efficiency coordination level

(a) Entropy production link optimization degree and cost-efficiency synergy degree

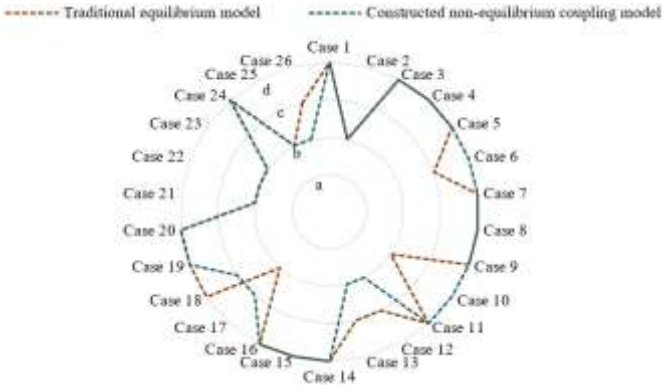

a: Load fluctuation adjustment adaptability level, b: Non-equilibrium degree control accuracy level c: Equipment adjustment response speed level, d: Distributed energy consumption coordination level

(b) Dynamic adjustment adaptability and non-equilibrium stability

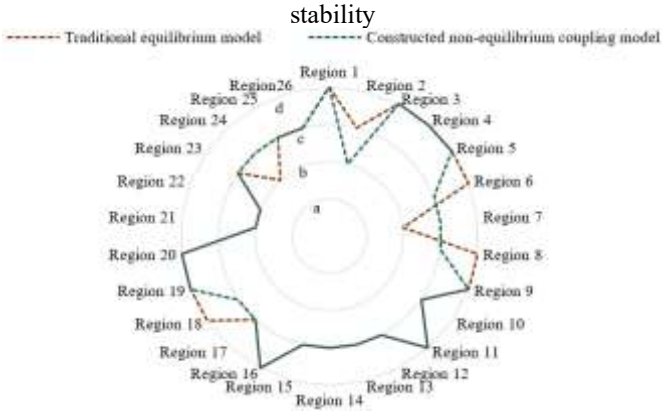

a: Initial operation efficiency level, b: Stable operation efficiency level, c: Long-term operation efficiency level, d: Optimal LCC level

(c) LCC deviation and non-equilibrium exergy efficiency

Figure 7. Comparison of non-equilibrium thermodynamic-economic coupling characteristics of typical regional energy system cases

This reflects the new model's precise regulation ability of irreversible losses in each stage. In the dynamic adjustment adaptability dimension, the new model performs better in indicators such as load fluctuation adaptability, non-equilibrium control accuracy, and equipment adjustment response speed. For example, distributed energy consumption coordination in commercial and residential systems such as Case 16 and Case 17 increases by nearly 30%, confirming the adaptability of the dynamic coupling regulation mechanism to condition fluctuations. In the lifecycle performance dimension, the new model's non-equilibrium exergy efficiency in the initial, stable, and long-term operation stages is higher than that of the traditional model, with an approximately 25% improvement in LCC optimization. In cases like Case 9 and Case 10, the long-term operation efficiency degradation is reduced from 20% in the traditional model to 8%, highlighting the new model's effective maintenance of non-equilibrium performance throughout the system's lifecycle. The above results fully support the core conclusion in the paper that "the constructed non-equilibrium coupling model can significantly improve the thermodynamic-economic coupling level of regional energy systems from three dimensions: entropy production regulation at the link level, dynamic condition adaptation, and lifecycle performance maintenance." This also demonstrates that the model has universal optimization capabilities that cover different types of regional energy systems.

5. CONCLUSION

This paper focuses on the essential nature of non-equilibrium states and the core demands of thermodynamic-economic coupling optimization in regional energy systems. It constructs a dynamic coupling model integrating non-equilibrium thermodynamics principles and lifecycle economic analysis. Through four core innovations—quantifying entropy production by stage, correcting non-equilibrium exergy efficiency, establishing the entropy production-cost mechanism relationship, and implementing the MPC dynamic adjustment mechanism—collaborative optimization of system comprehensive performance under non-equilibrium states is achieved. Empirical results show that the proposed model reduces LCC by 8.9% compared to traditional equilibrium coupling models. The average absolute error between non-equilibrium exergy efficiency and measured values is controlled within 1.18%, with R^2 values above 0.92, demonstrating significant accuracy improvements over the traditional model. The impact weight of non-equilibrium degree on coupling optimization results is 28%, the entropy production optimization rate in the energy conversion and transmission stages exceeds 40%, and the dynamic adjustment error in medium load fluctuation scenarios can be reduced to around -10. This fully confirms the central role of non-equilibrium characteristics in system optimization and the adaptability of the dynamic coupling mechanism to working conditions. The theoretical value of this research lies in breaking through the limitations of equilibrium assumptions in system-level coupling analysis, extending non-equilibrium thermodynamics theory from individual devices to regional energy systems, and establishing a complete analytical framework of "non-equilibrium state representation - mechanism coupling - dynamic optimization." The engineering value is reflected in providing a quantitative tool with both accuracy and general applicability, which can directly support equipment selection, pipeline layout, and operational strategy optimization for regional energy systems, offering a clear basis for balancing investment costs and operational benefits.

Although this study has achieved stage results in model construction and empirical verification, there are still three limitations that need further expansion: 1) The case study focuses on urban new districts in China's temperate regions, and the applicability to extreme climate zones such as cold,

hot summer and warm winter areas, and specific scenarios like pure industrial or ultra-large parks has not been fully verified; 2) The model parameter calibration relies on ideal operating condition equipment experimental data, and the depiction of long-term irreversible degradation processes such as equipment aging and pipeline scaling still needs to be deepened; 3) The real-time verification of the dynamic adjustment mechanism is based on simulation analysis, lacking actual operating data support from semi-physical simulations or engineering demonstrations. Future research can advance in three areas: expanding the case coverage to include regional energy systems in different climate zones and with different load types to further improve model generalization ability; introducing equipment lifecycle degradation models and uncertainty analysis methods, considering random factors such as energy price fluctuations and sudden meteorological changes, to enhance model robustness; integrating digital twin technology to build a real-time optimization platform that combines virtual and physical systems, verifying the actual operating effects of the dynamic coupling adjustment mechanism through engineering demonstrations, and deepening the study of non-equilibrium state evolution and multi-physics field coupling micro-mechanisms to provide more solid theoretical support for the low-carbon, efficient operation of regional energy systems.

REFERENCES

[1] Mikulandrić, R., Krajačić, G., Duić, N., Khavin, G., Lund, H., Vad Mathiesen, B., Østergaard, P. (2015). Performance analysis of a hybrid district heating system: A case study of a small town in Croatia. Journal of Sustainable Development of Energy, Water and Environment Systems, 3(3): 282-302. https://doi.org/10.13044/j.sdewes.2015.03.0022

[2] Kayayan, V.A., Cabral, D., Israelsson, K., Gustafsson, M. (2025). Positive energy districts in Sweden: The impact from heat Pumps, photovoltaic Systems, and energy recovery from district heating return pipe. Energy and Buildings, 334: 115471. https://doi.org/10.1016/j.enbuild.2025.115471

[3] Zhang, X., Lyu, J., Wang, Z., Li, Y., Deng, K., Dehghanian, P., Chen, B. (2025). Low carbon regional energy management system with conditional value at risk. Journal of Building Engineering, 107: 112572. https://doi.org/10.1016/j.jobe.2025.112572

[4] Viholainen, J., Luoranen, M., Väisänen, S., Niskanen, A., Horttanainen, M., Soukka, R. (2016). Regional level approach for increasing energy efficiency. Applied Energy, 163: 295-303. https://doi.org/10.1016/j.apenergy.2015.10.101

[5] Haldar, S., Bhandari, P., Chakraborty, S. (2017). Emergent Scenario in first and second order non-equilibrium thermodynamics and stability analysis. Annals of Physics, 387: 203-212. https://doi.org/10.1016/j.aop.2017.10.013

[6] Shen, H.C. (2005). Application of analytical thermodynamics: Relativistic transformation of temperature in equilibrium thermodynamics. Acta Physica Sinica, 54(6): 2482-2488.

[7] Nery, A.R.L., Bassi, A.B.M.S. (2011). Conditions for thermodynamic equilibrium: the function availability. Química Nova, 34: 160-164. https://doi.org/10.1590/S0100-40422011000100030

[8] Pang, L., Zhao, M., Luo, K., Yin, Y., Yue, Z. (2018). Dynamic temperature prediction of electronic equipment under high altitude long endurance conditions. Chinese Journal of Aeronautics, 31(6): 1189-1197. https://doi.org/10.1016/j.cja.2018.04.002

[9] Michaelides, E.E. (2012). Entropy production and optimization of geothermal power plants. Journal of Non-Equilibrium Thermodynamics, 37(3): 233-246. https://doi.org/10.1515/jnetdy-2011-0024

[10] Sun, X., Zhang, W., Kuang, X. (2024). Radiation effect or siphon effect? Coupled coordination and spatial effects of digital economy and green manufacturing efficiency—Evidence from spatial Durbin modelling. PloS One, 19(11): e0313654. https://doi.org/10.1371/journal.pone.0313654

[11] Redo, M.A., Giannetti, N., Yoshimura, H., Saito, K., Watanabe, M. (2022). Development and validation of a variational formulation of Two-Phase flow distribution. International Journal of Multiphase Flow, 155: 104190. https://doi.org/10.1016/j.ijmultiphaseflow.2022.104190

[12] Kang, D., Yu, J., Lv, G., Ma, W., Gu, X., Xiong, C., Liu, H. (2019). Numerical research on carbon activity, fuel utilization, chemical reaction, and temperature distribution for IT single planar SOFC. Energy Sources, Part A: Recovery, Utilization, and Environmental Effects, 41(1): 94-104. https://doi.org/10.1080/15567036.2018.1496200

[13] Tsai, C.T., Peng, F.W. (2023). Design and implementation of charging and discharging management system for two-set lithium ferrous phosphate batteries. Sensors and Materials, 35(4): 1255. https://doi.org/10.18494/SAM4119

[14] Samui, A., Samantaray, S.R. (2013). Wavelet singular entropy-based islanding detection in distributed generation. IEEE Transactions on Power Delivery, 28(1): 411-418. https://doi.org/10.1109/TPWRD.2012.2220987

[15] Mao, Y., Cai, L., Chertovskih, R., Ji, J., Su, S. (2025). Working characteristics of the scroll expander for residual pressure recovery in microscale gas pipeline networks. Machines, 13(3): 196. https://doi.org/10.3390/machines13030196

[16] Devlin, A., Yang, A. (2022). Regional supply chains for decarbonising steel: Energy efficiency and green premium mitigation. Energy Conversion and Management, 254: 115268. https://doi.org/10.1016/j.enconman.2022.115268

[17] Huang, Z., Fang, Z., Lam, C.S., Mak, P.I., Martins, R.P. (2019). Cost-effective compensation design for output customization and efficiency optimization in series/series-parallel inductive power transfer converter. IEEE Transactions on Industrial Electronics, 67(12): 10356-10365. https://doi.org/10.1109/TIE.2019.2959491

[18] Farafonova, N.V. (2011). Essence and components of economic efficiency of business activities within agrarian sector. Actual Problems of Economics, (124): 176-185.

[19] Kumari, G.G., Abdufattokhov, S., Singh, S., Aradhya S,G.B., et al. (2025). Leveraging LSTM-Driven predictive analytics for resource allocation and cost efficiency optimization in project management. International Journal of Advanced Computer Science &

Applications, 16(6): 621-629. https://doi.org/10.14569/ijacsa.2025.0160661
[20] Lin, Y., Yang, W. (2018). Application of multi-objective genetic algorithm based simulation for cost-effective building energy efficiency design and thermal comfort improvement. Frontiers in Energy Research, 6: 25. https://doi.org/10.3389/fenrg.2018.00025